

Rapid Holocene Deglaciation of the Labrador Sector of the Laurentide Ice Sheet

ANDERS E. CARLSON* AND PETER U. CLARK

Department of Geosciences, Oregon State University, Corvallis, Oregon

GRANT M. RAISBECK

Centre de Spectrométrie Nucléaire et de Spectrométrie de Masse, IN₂P₃/CNRS, Orsay, France

EDWARD J. BROOK

Department of Geosciences, Oregon State University, Corvallis, Oregon

(Manuscript received 29 August 2006, in final form 31 January 2007)

ABSTRACT

Retreat of the Laurentide Ice Sheet (LIS) following the Last Glacial Maximum 21 000 yr BP affected regional to global climate and accounted for the largest proportion of sea level rise. Although the late Pleistocene LIS retreat chronology is relatively well constrained, its Holocene chronology remains poorly dated, limiting our understanding of its role in Holocene climate change and sea level rise. Here new ¹⁰Be cosmogenic exposure ages on glacially deposited boulders are used to date the final disappearance of the Labrador sector of the LIS (LS-LIS). These data suggest that following the deglaciation of the southeastern Hudson Bay coastline at 8.0 ± 0.2 cal ka BP, the southwestern margin of the LS-LIS rapidly retreated ~ 600 km in 140 yr and most likely in ~ 600 yr at a rate of ~ 900 m yr⁻¹, with final deglaciation by 6.8 ± 0.2 ¹⁰Be ka. The disappearance of the LS-LIS ~ 6.8 ¹⁰Be ka and attendant reduction in freshwater runoff may have induced the formation of Labrador Deep Seawater, while the loss of the high albedo surface may have initiated the Holocene Thermal Maximum in eastern Canada and southern Greenland. Moreover, the rapid melting just prior to ~ 6.8 ¹⁰Be ka indicates that the remnant LIS may be the primary source of a postulated rapid rise in global sea level of ~ 5 m that occurred sometime between 7.6 and 6.5 cal ka BP.

1. Introduction

The Laurentide Ice Sheet (LIS) was the largest of the former Northern Hemisphere ice sheets and had a significant effect on climate and sea level during the last glaciation (Clark et al. 1999). Over the area of North America that was glaciated by the LIS, ice sheet retreat caused 1) a weakening of high pressure centered over the ice sheet and attendant changes in atmospheric circulation, 2) warmer temperatures induced by the reduced height and extent of its high albedo surface, and

3) a decrease in precipitation minus evaporation (Mitchell et al. 1988; Bartlein et al. 1998; Kutzbach et al. 1998; Pollard et al. 1998). Additionally, retreat of the LIS accounted for the largest proportion of the deglacial sea level rise, and associated freshwater fluxes to the North Atlantic Ocean may have affected the Atlantic meridional overturning circulation.

Understanding the role of the LIS in climate and sea level change requires a well-dated chronology of changes in its spatial dimensions. Although the retreat chronology of the LIS during the late Pleistocene (21–11.5 ka BP) is relatively well constrained by hundreds of ¹⁴C dates and extensive moraines that document the age and position of the retreating ice margin, its subsequent Holocene retreat history remains poorly known with the exception of the Baffin Island/Foxe Basin region (Fig. 1) (Dyke 2004; Miller et al. 2005). The existing Holocene chronology captures the gross pattern of deglaciation, including ice-margin retreat toward the three main centers of mass (Labrador, Keewatin, and

* Current affiliation: Department of Geology and Geophysics, University of Wisconsin—Madison, Madison, Wisconsin.

Corresponding author address: Anders E. Carlson, Department of Geology and Geophysics, University of Wisconsin—Madison, 1215 W. Dayton St., Madison, WI 53706.
E-mail: acarlson@geology.wisc.edu

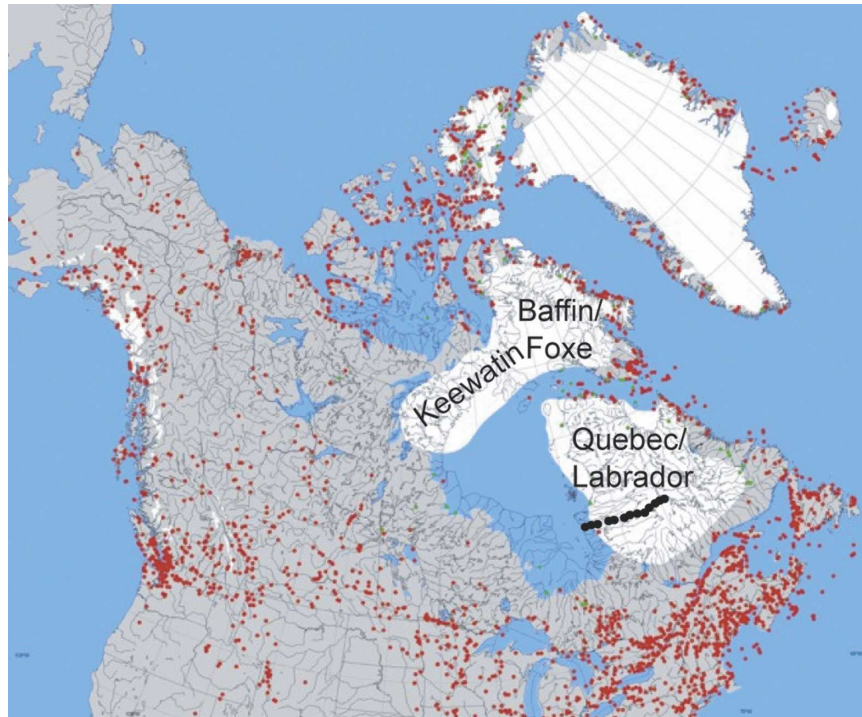


FIG. 1. Sample locations (black dots) overlain on the 7.6 ^{14}C ka BP (8.4 cal ka BP) map of Dyke (2004) with three remaining ice caps labeled. Red dots are minimum-limiting radiocarbon greater than or equal to 8.4 cal ka BP; green dots are radiocarbon ages that provide a 300-yr range from just after 8.4 cal ka BP (8.4 to 8.1 cal ka BP).

Baffin Island/Foxe Basin), and the opening of Hudson Bay ~ 8.4 cal ka BP (Barber et al. 1999), which caused the LIS to fragment into three ice caps that were remnants of the three originally coalescent ice centers (Fig. 1). In general, however, the details of Holocene deglaciation of the LIS remain poorly constrained outside of the Baffin Island/Foxe Basin region, largely because most of the few available ^{14}C ages are considered unreliable (Dyke 2004).

We address these issues by developing a chronology for the final retreat of the Labrador sector of the LIS (LS-LIS), which was the largest of the three remaining ice caps, using cosmogenic ^{10}Be exposure ages from boulders sampled along a transect across north-central Quebec (Fig. 1). While ^{10}Be dates are analytically less precise than radiocarbon dates, cosmogenic ages directly date the actual timing of deglaciation, whereas radiocarbon ages date the arrival of vegetation to a region sometime after deglaciation. Radiocarbon ages are also restricted by the availability of lakes for coring and the assumption that the bottom of the lake sediments was reached. Furthermore, bulk radiocarbon ages in northeastern Canada have an inherent problem of contamination by old carbon (Short and Nichols 1977; Dyke 2004) reducing their accuracy. Currently,

the timing of the marine limit and eight minimum limiting bulk radiocarbon ages, only four of which are near the inferred ice margin, constrain the retreat of the LS-LIS in north-central Quebec (Hardy 1976; Dyke 2004). Our new chronology thus represents a significant improvement over the existing limited radiocarbon chronology (Dyke 2004) in constraining the final disappearance of the LS-LIS and its relationship to Holocene climate change and sea level rise.

2. Methods

We sampled 13 granitic or gneissic Precambrian boulders along an ~ 650 km long transect parallel to the general retreat direction of the western margin of the LS-LIS from the coast of James Bay to near the Quebec-Labrador border, providing a spatial resolution of about one sample every 50 km and a relatively continuous record of ice retreat (Fig. 1). This transect was accessed via the Canadian Highway linking hydroelectric dams on the La Grande River. We only sampled isolated boulders on bedrock highs that were greater than 1 m in height in order to reduce the possibility of snow cover (Table 1). None of our boulders were shielded significantly by the surrounding topography.

TABLE 1. Sample characteristics, ^{10}Be concentration, scaling factors, age, and error. All samples were 1 cm thick. An attenuation length of 150 g cm^{-2} and density of 2.8 g cm^{-3} were used to scale sample thickness; 50 g of pure quartz was dissolved for each sample. Measured blanks yielded no counts and were thus assumed negligible relative to measured concentrations. One-sigma error is calculated from counting statistics and 5% machine error.

Sample	Altitude (m)	Latitude ($^{\circ}\text{N}$)	Longitude ($^{\circ}\text{W}$)	Boulder height (m)	$[^{10}\text{Be}]$ (atoms g^{-1})	Latitude and altitude scaling factor	Time average scaling factor	Age (yr)	1σ error
QC-2	136	53.695	78.096	1	32 886	1.16	1.06	7000	770
QC-4	167	53.384	77.527	1	39 900	1.19	1.09	8200	760
QC-6	200	53.538	76.497	2	37 719	1.23	1.13	7500	630
QC-10	299	53.528	74.871	1	44 430	1.36	1.25	7900	920
QC-11	327	53.552	74.479	1.5	40 943	1.40	1.31	7000	590
QC-13	467	53.834	73.5	1.5	44 900	1.60	1.50	6700	580
QC-15	434	53.849	72.678	2	42 500	1.55	1.45	6500	570
QC-27	460	53.984	72.057	1	44 027	1.59	1.49	6600	590
QC-17	485	54.042	71.788	1.5	43 369	1.63	1.53	6400	550
QC-19	519	54.195	71.479	1.5	45 839	1.68	1.58	6500	670
QC-23	509	54.474	70.58	1	53 131	1.66	1.56	7600	650
QC-24	606	54.688	70.273	1.2	49 559	1.82	1.72	6500	550
QC-25	669	54.785	69.982	1.2	66 441	1.92	1.82	8200	1100

All samples were from the top 1 cm from the center of horizontal surfaces on the highest part of each boulder in order to minimize the attenuation correction for cosmogenic nuclide production with depth. Each sampled boulder showed evidence of glacial abrasion such as polish and striae, indicating removal of previously exposed surfaces and absence of significant postglacial erosion. The Quebec/Labrador region experienced extensive periods of erosive, wet-based ice cover during the last glacial period, as reflected by numerous ice flow indicators eroded into the bedrock surface (Veillette et al. 1999), suggesting that the effects of inherited ^{10}Be are minimized in our samples.

Targets were prepared for accelerator mass spectrometry (AMS) following the procedures of Licciardi (2000) and Rinterknecht (2003), and $^{10}\text{Be}/^9\text{Be}$ ratios were measured at the AMS facility at Gif sur Yvette, France (Raisbeck et al. 1994) relative to National Institute of Standards and Technology (NIST) standard 4325, using the certified ratio of 2.68×10^{-11} . Ages were calculated using the production rate of $5.1\text{ }^{10}\text{Be}$ atoms $\text{g}^{-1}\text{ yr}^{-1}$ at sea level and high latitude (Stone 2000), scaled for latitude and altitude according to Lal (1991) and Stone (2000), and reduced by 14% because of the different standard used in these measurements compared to that used to make the production rate measurements (Middleton et al. 1993).

Following the method used by Rinterknecht et al. (2004), we corrected our data for the considerable isostatic uplift that our samples have experienced since deglaciation (Fig. 2a). We determined the elevation history of each boulder following deglaciation using the isostatic maps of Andrews and Peltier (1989) and rela-

tive sea level curves of Hardy (1976) and Mitrovica et al. (2000). We convert this history into a time-varying production scaling factor and then calculate the time-averaged scaling factor. This decreases our production scaling factor by 5%–8% (Fig. 2a, Table 1). In addition, our three samples closest to James Bay experienced initial cover by seawater due to isostatic submergence and high relative sea level. Given the 90% reduction in production cosmogenic nuclides at a depth of 5 m below sea level, we thus assume that these boulders date the emergence of the coastline due to isostatic rebound rather than deglaciation.

We calculated 1σ error using counting statistics and a conservative 5% machine error (long-term variability in the standards). We did not propagate any additional error involved in the production rate or scaling factors. In comparing ^{10}Be years to calendar years (cal yr), there is an additional uncertainty ($\sim 10\%$) involved in the production rate calibration, isostatic correction, and scaling factors.

3. Results

Because the exposure ages on our three westernmost samples (QC-2, 4, and 6; Table 1) date isostatic emergence from seawater rather than initial deglaciation, we treat them separately from those samples farther to the east that date deglaciation. These three ages are in good agreement (at 2σ) with the calibrated radiocarbon ages that constrain the postglacial emergence history of the James Bay coast (Hardy 1976) (Fig. 2b). The age of the highest marine shoreline (marine limit) from a reservoir corrected, calibrated mollusk shell in-

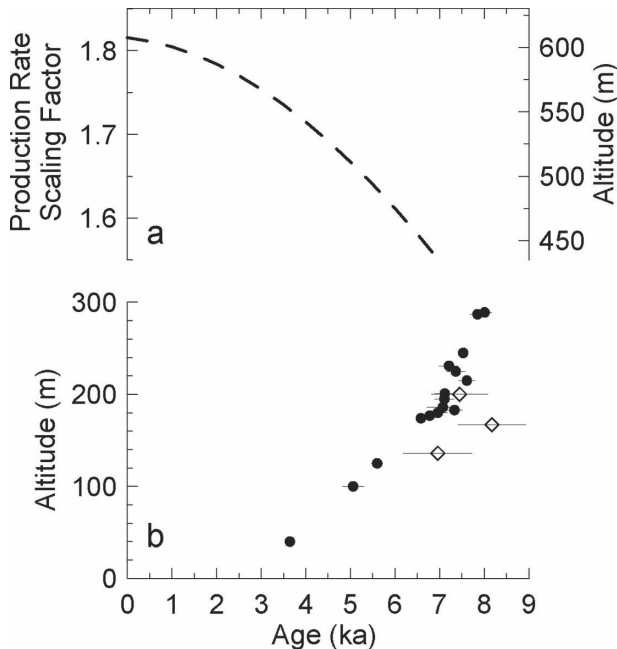


FIG. 2. Isostatic adjustment data and relative sea level history. (a) Change in the production rate scaling factor through time due to isostatic uplift (for sample QC-24) using the procedure of Rinterknecht et al. (2004). (b) Relative sea level history for eastern James Bay. Solid circles are ^{14}C ages from Hardy (1976) calibrated using a ΔR of 310 ± 50 yr (Barber et al. 1999) and CALIB 5.01 (1σ error bars shown); open diamonds are ^{10}Be ages (1σ error bars shown).

dicates that deglaciation of this part of the James Bay coastline occurred 8.0 ± 0.2 cal ka BP.

The second group consists of our remaining 10 samples that date deglaciation as the ice margin retreated to the east. Because these samples overlap at the 2σ uncertainty level (Table 1, Fig. 3a), we are unable to exclude any one sample from the population despite the suggestion of two older dates in the east (QC-23 and QC-25). All of the ages are also statistically indistinguishable from the mean of sample ages at 1σ .

There is the suggestion of a west-to-east trend in this sample group, and a linear fit to the data including the timing of the marine limit suggests that retreat occurred between 7.4 and 6.8 ^{10}Be ka in ~ 600 yr with a corresponding retreat rate of ~ 900 m yr^{-1} (Fig. 3a). Although the R^2 value (0.08, $P = 0.37$) indicates no statistical significance to this fit, it still implies very rapid to essentially instantaneous retreat. To estimate the actual timing of deglaciation, we calculate an error-weighted mean age of 6.8 ± 0.2 ^{10}Be ka (at 1σ) from this statistically indistinguishable group (Fig. 3). We report the error-weighted mean age because the standard deviation of the mean of sample ages (665 yr) is about what is expected from the average analytical er-

ror (685 yr) (Bevington and Robinson 2002). We determine the error of this mean age ($1\sigma = \pm 0.2$ ^{10}Be ka) using the standard error of the dataset (Bevington and Robinson 2002).

In addition to a linear fit, we also use Monte Carlo retreat simulations to calculate the timing of ice margin retreat for this second group of samples, including the timing of the marine limit. We generated 3000 possible retreat scenarios assuming a normal distribution with the analytical uncertainty centered on each sample age. From these scenarios, we arrive at the average or most recurring retreat rate, providing an estimate for the duration of retreat. The results of the Monte Carlo simulations suggest that the LS-LIS deglaciated in 620 ± 760 yr, in agreement with the ~ 600 yr suggested by the linear fit to the data.

The ^{10}Be age of deglaciation at 6.8 ± 0.2 ^{10}Be ka is bracketed by the two bulk radiocarbon dates of 7.29 ± 0.14 and 6.31 ± 0.05 cal ka BP on gyttja at 70° to 69°W (Dyke 2004) (Fig. 3a). Another five bulk radiocarbon ages at 73°W on gyttja and lake sediment place ice retreat sometime before 6.52 ± 0.14 to 7.50 ± 0.07 cal ka BP (Dyke 2004) (Fig. 3a). The variability in these bulk radiocarbon dates and possibility of old carbon contamination makes inferring the timing of deglaciation from these radiocarbon dates difficult, but the dates do bracket our ^{10}Be chronology and the age we calculate for deglaciation.

Our calculated retreat rate is also considerably faster than the one established from the existing radiocarbon compilation chronology (Dyke 2004), which suggests a more gradual eastward recession of the ice margin from 8.4 to 6.0 cal ka BP. In particular, our data suggest that, following deglaciation of the northeastern James Bay coast 8.0 ± 0.2 cal ka BP, the western margin of the LS-LIS remained semistationary before beginning a rapid retreat ~ 7.4 to 7.0 ^{10}Be ka. Thus, our ^{10}Be ages provide a more accurate record of the time of deglaciation because they date the initial exposure of a boulder following deglaciation versus radiocarbon ages, which date the arrival and accumulation of vegetation with an inherent possibility of old carbon contamination.

4. Discussion

Our ^{10}Be ages provide the first direct dating of the retreat of the LS-LIS. These data suggest that, following deglaciation of the coastline at 8.0 ± 0.2 cal ka BP (age of the marine limit) (Fig. 2b), the LS-LIS disintegrated rapidly just before 6.8 ± 0.2 ^{10}Be ka (Fig. 3). The rapid deglaciation of the center of the LIS over Hudson Bay between 9.0 and 8.4 cal ka BP was likely caused by

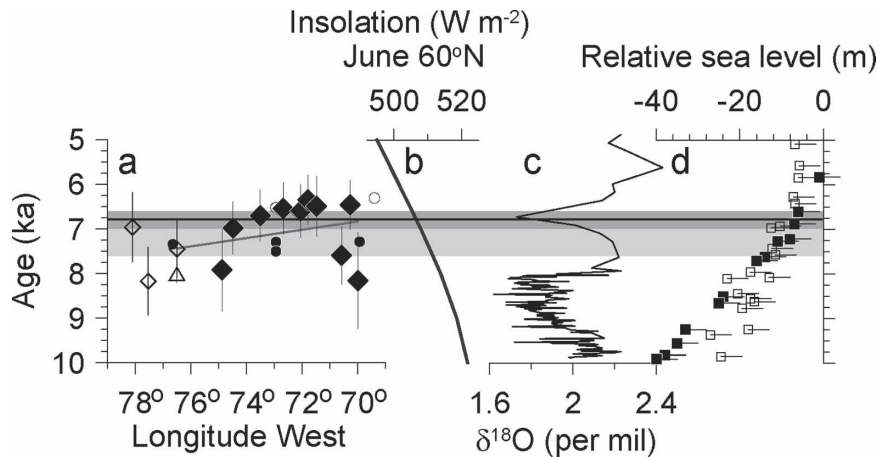


FIG. 3. The ^{10}Be chronology for the western margin of the Labrador sector of the Laurentide Ice Sheet, deglaciation forcing, planktonic Labrador Sea $\delta^{18}\text{O}$, and relative sea level data. Dark gray bar denotes the error-weighted mean age of collapse of the Labrador sector Ice Cap at 6.8 ^{10}Be ka with 1σ standard error (± 0.2 ^{10}Be ka); the light gray bar indicates the postulated rapid sea level rise from 7.6 to 6.9 cal ka BP (Blanchon and Shaw 1995). (a) ^{10}Be ages with 1σ error bars (open diamonds date the emergence of the coast; filled diamonds date deglaciation) (see Fig. 1 for sample location). Open triangle is the timing of the marine limit (see Fig. 2). Line is the linear fit ($R^2 = 0.08$) to the deglacial ^{10}Be ages (filled diamonds) and marine limit (open triangle). Calibrated radiocarbon dates from the 6.5 ^{14}C ka (7.45 cal ka BP) map (open circles) and the 6.0 ^{14}C ka (6.8 cal ka BP) map (closed circles) of Dyke (2004). (b) June insolation at 60°N (Berger and Loutre 1991). (c) *G. bulloides* $\delta^{18}\text{O}$ record from the Labrador Sea (Hillaire-Marcel et al. 2001). (d) Relative sea level data: closed squares from Tahiti (Bard et al. 1996) and open squares from the Caribbean (Lighty et al. 1982) (recalibrated using CALIB 5.01). The 1σ age error bars are shown along with the growth habitat of the corals.

an extensive calving margin associated with proglacial lakes and marine incursion up Hudson Strait (Barber et al. 1999; Dyke 2004). Calving cannot explain the rapid collapse of the LS-LIS ~ 6.8 ^{10}Be ka, however, because the ice margin was land based at that time. Instead, we attribute the rapid margin retreat to top-down melting induced by a large rise in the equilibrium line altitude (ELA). Such a rapid rise in the ELA may have been in response to the deglaciation of Hudson Bay ice, which would have reorganized regional atmospheric circulation and induced warming through the increase in the thermal capacity of Hudson Bay seawater relative to ice. However, the atmospheric effects of this would be immediate with only a slight lag in the seawater effects, and the LS-LIS remained near the western coast from 8.4 to 8.0 ka with only minor inland retreat until ~ 7.4 to 7.6 ka when it rapidly retreated.

Another possible explanation for the abrupt rise in ELA involves the persistence of ice over eastern Keewatin, west of Hudson Bay, and Foxe Basin, north of Hudson Bay (Fig. 1), which would produce a regional high pressure system that could deflect the summer westerlies south of the LS-LIS. Accordingly, the northward migration of this seasonally warm air mass follow-

ing deglaciation of Keewatin and Foxe Basin could have caused the rapid rise in ELA. However, the timing of ice retreat in Keewatin is poorly constrained by only four minimum limiting radiocarbon dates, three of which are far removed from the ice margin (Dyke 2004), and the corresponding chronology of deglaciation (sometime after 8.0 to 6.8 cal ka BP) is indistinguishable from that of the LS-LIS. The deglaciation of Foxe Basin is constrained by 11 minimum limiting radiocarbon dates, with retreat commencing after 7.8 cal ka BP and complete by 7.45 to 6.8 cal ka BP, also indistinguishable from that of the LS-LIS (Dyke 2004).

We modeled the inferred response of the LS-LIS to a rise in the ELA using a positive-degree-day model that calculates ice thickness (h in meters) as a function of the difference between the original ice thickness (h_0 in meters) and net mass balance b_n (in m yr^{-1}), which depends on the ice thickness h and time (t in years):

$$h(t) = h_0 - \int_0^t b_n(h, t) dt.$$

We initialize the ice thickness (2320 m) to be the same as that determined by an ice sheet model (Licciardi et

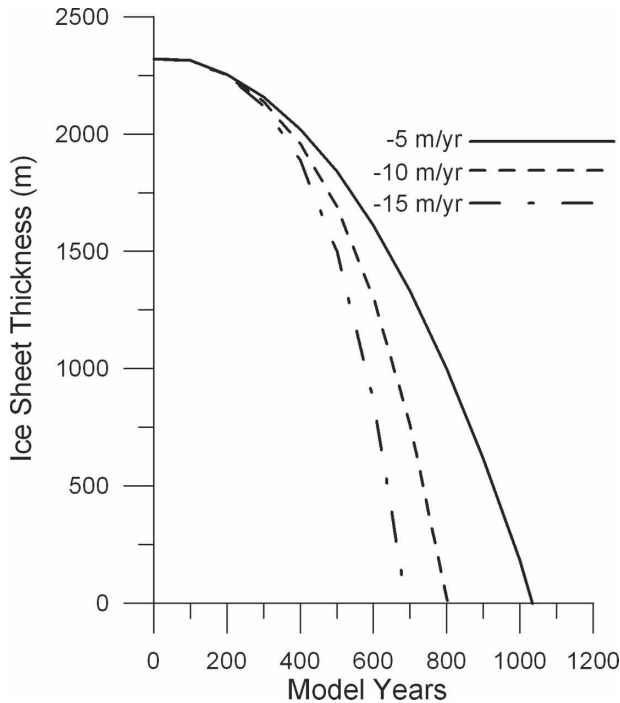


FIG. 4. Positive-degree-day model results for the center of the ice sheet. The terminus b_n rates for model simulations are as follows: the solid line is $-5 \text{ m yr}^{-1} b_n$, the dashed line is $-10 \text{ m yr}^{-1} b_n$, and the dashed-dotted line is $-15 \text{ m yr}^{-1} b_n$.

al. 1998). Mass balance increases linearly with elevation and decreases linearly with time as more ice (lower albedo and rougher surface than snow) is exposed. The model does not include ice dynamics, which would cause faster draw down of the ice surface, making this model a conservative treatment of the deglaciation process. Using reasonable b_n values for an ice sheet without an accumulation zone (-5 to -15 m yr^{-1} at the terminus increasing to -0.1 m yr^{-1} at 2320-m ice thickness), the model suggests that the LS-LIS could have melted within $860 \pm 170 \text{ yr}$ (Fig. 4), in good agreement with the estimated retreat time based on our Monte Carlo simulations of the ^{10}Be ages and the linear fit to the ages (Fig. 3a).

Simulations with numerical climate models indicate that removal of the LIS would induce warming over eastern North America to northern Europe (Mitchell et al. 1988; Pollard et al. 1998; Renssen et al. 2005). In support of this, paleoclimate records show a delayed onset of the Holocene Thermal Maximum (HTM) between 7 and 6 cal ka BP over central and northeastern North America and southern Greenland, lagging behind the HTM onset in Alaska, Arctic Canada, and northern Greenland of 11.0 to 8.0 cal ka BP (Kaufman et al. 2004; Kaplan and Wolfe 2006). This indicates that the remnant LIS delayed the insolation-induced HTM

across the western Atlantic and lower Arctic latitudes by up to 4000 yr relative to the insolation maximum at $\sim 11 \text{ ka BP}$ (Fig. 3b) through the attendant cooling associated with its high albedo.

Our results also suggest that rapid melting of the LS-LIS between 8.0 and 6.8 ^{10}Be ka and most likely between 7.4 and 6.8 ^{10}Be ka may be the primary source for a postulated interval of rapid global sea level rise of $\sim 5 \text{ m}$ that occurred sometime between 7.6 to 6.5 cal ka BP (Fig. 3) (Blanchon and Shaw 1995). Blanchon and Shaw (1995) attributed this meltwater pulse (mwp) to an Antarctic source, but, at least for the West Antarctic Ice Sheet, ice sheet thinning did not accelerate until after 7.0 cal ka BP (Conway et al. 1999; Stone et al. 2003), indicating that this ice sheet did not contribute significantly to the event. The exact timing and rate of this mwp is uncertain, with coral data from Tahiti indicating that the event occurred between 7.6 to 6.9 cal ka BP at a rate of $\sim 10 \text{ mm yr}^{-1}$ (Bard et al. 1996; Montaggioni et al. 1997), whereas coral data from the Caribbean (Lighty et al. 1982) suggest it occurred between 7.0 to 6.5 cal ka BP at a rate of $>45 \text{ mm yr}^{-1}$ (Blanchon and Shaw 1995) (Fig. 3). Nevertheless, within dating uncertainties, our data suggest that the period of rapid melting of the LS-LIS would have contributed $\sim 3 \text{ m}$ (Licciardi et al. 1998) to the mwp. The additional 2 m of sea level rise during this period may be mainly sourced from the Keewatin sector, which deglaciated by 8.0 to 6.8 cal ka BP (Dyke 2004), and the Baffin Island/Foxe Basin sector of the LIS (Dyke 2004; Miller et al. 2005). Any additional sea level rise after 7.0 cal ka BP must then be attributed to the continued deglaciation of Antarctica (Stone et al. 2003) and the $\sim 1 \text{ m}$ of sea level rise remaining in the Baffin Island/Foxe Basin sector (Licciardi et al. 1998), which continued to deglaciate through the remainder of the Holocene (Miller et al. 2005).

The disappearance of the LS-LIS at $6.8 \pm 0.2 \text{ }^{10}\text{Be}$ ka is coincident with the initiation of Labrador "Deep Seawater" (LDSW) formation at $\sim 7.0 \text{ cal ka BP}$ (Hillaire-Marcel et al. 2001). We postulate that melting of the LS-LIS up to 6.8 ^{10}Be ka may have freshened and stratified the Labrador Sea, thus preventing the formation of LDSW (Cottet-Puinel et al. 2004). The enhanced freshwater flux associated with the final rapid melting may be recorded by a light planktonic foraminifer $\delta^{18}\text{O}$ anomaly in the Labrador Sea (Fig. 3) (Hillaire-Marcel et al. 2001). The subsequent disappearance of the majority of the LIS allowed the establishment of a more saline surface water mass in the Labrador Sea $\sim 7.0 \text{ cal ka BP}$ (Solignac et al. 2004), which would allow convection and LDSW formation. Retreat of the Greenland ice sheet (GIS) may also have contributed to fresh-

ening of the Labrador Sea, but this is likely of a much smaller magnitude because the glacial–interglacial adjustment of the GIS was largely complete by the early Holocene (~10 to 8 cal ka BP) (Bennike and Björck 2002). The initiation of LDSW and attendant heat dissipation to the atmosphere may then have been an important feedback to the warming associated with the HTM in eastern Canada and Greenland.

Acknowledgments. We thank A. Carlson for help in the field, and F. Anslow, L. Ersek, B. Goehring, K. Lake, and V. Rinterknecht for discussions and help in the lab. Reviews by M. Kaplan, J. Licciardi, S. Marshall, and one anonymous reviewer greatly improved the manuscript. This research was supported by grants from NSF (BCS-0402325, A.E.C. and P.U.C.) and GSA (A.E.C.). Tandetron operation is supported by the IN₂P₃ and INSU divisions of the CNRS.

REFERENCES

- Andrews, J. T., and W. R. Peltier, 1989: Quaternary geodynamics in Canada. *Quaternary Geology of Canada and Greenland*, R. J. Fulton, Ed., Vol. K-1, *Geology of North America*, Canadian Government Publishing Centre, 541–572.
- Barber, D. C., and Coauthors, 1999: Forcing of the cold event of 8,200 years ago by catastrophic drainage of Laurentide lakes. *Nature*, **400**, 344–348.
- Bard, E., B. Hamelin, A. Maurice, L. F. Montaggioni, G. Cabioch, G. Faure, and F. Rougerie, 1996: Deglacial sea-level record from Tahiti corals and the timing of global meltwater discharge. *Nature*, **382**, 241–244.
- Bartlein, P. J., and Coauthors, 1998: Paleoclimate simulations for North America over the past 21,000 years: Features of the simulated climate and comparisons with paleoenvironmental data. *Quat. Sci. Rev.*, **17**, 549–585.
- Bennike, O., and S. Björck, 2002: Chronology of the last recession of the Greenland Ice Sheet. *J. Quat. Sci.*, **17**, 211–219.
- Berger, A., and M. F. Loutre, 1991: Insolation values for the climate of the last 10 million years. *Quat. Sci. Rev.*, **10**, 297–317.
- Bevington, P., and D. K. Robinson, 2002: *Data Reduction and Error Analysis for the Physical Sciences*. 3d ed. McGraw-Hill, 336 pp.
- Blanchon, P., and J. Shaw, 1995: Reef drowning during the last deglaciation: Evidence for catastrophic sea-level rise and ice-sheet collapse. *Geology*, **23**, 4–8.
- Clark, P. U., R. B. Alley, and D. Pollard, 1999: Northern Hemisphere ice-sheet influences on global climate change. *Science*, **286**, 1104–1111.
- Conway, H., B. L. Hall, G. H. Denton, A. M. Gades, and E. D. Waddington, 1999: Past and future grounding-line retreat of the West Antarctic Ice Sheet. *Science*, **286**, 280–283.
- Cottet-Puinel, M., A. J. Weaver, C. Hillaire-Marcel, A. de Vernal, P. U. Clark, and M. Eby, 2004: Variation of Labrador Sea Water formation over the Last Glacial cycle in a climate model of intermediate complexity. *Quat. Sci. Rev.*, **23**, 449–465.
- Dyke, A. S., 2004: An outline of North American Deglaciation with emphasis on central and northern Canada. *Quaternary Glaciations-Extent and Chronology, Part II: North America*, Vol. 2b. J. Ehlers and P. L. Gibbard, Eds., Elsevier Science and Technology Books, 373–424.
- Hardy, L., 1976: Contribution à l'étude géomorphologique de la portion Québécoise de la Baie de James. Ph.D. thesis, McGill University, 264 pp.
- Hillaire-Marcel, C., A. de Vernal, G. Bilodeau, and A. J. Weaver, 2001: Absence of deep-water formation in the Labrador Sea during the last interglacial period. *Nature*, **410**, 1073–1077.
- Kaplan, M. R., and A. P. Wolfe, 2006: Spatial and temporal variability of Holocene temperature in the North Atlantic region. *Quat. Res.*, **65**, 223–231.
- Kaufman, D. S., and Coauthors, 2004: Holocene thermal maximum in the western Arctic (0–180°W). *Quat. Sci. Rev.*, **23**, 529–560.
- Kutzbach, J., R. Gallimore, S. Harrison, P. Behling, R. Selin, and F. Laarif, 1998: Climate and biome simulations for the past 21,000 years. *Quat. Sci. Rev.*, **17**, 473–506.
- Lal, D., 1991: Cosmic ray labeling of erosion surfaces: In situ nuclide production rates and erosion models. *Earth Planet. Sci. Lett.*, **104**, 424–439.
- Licciardi, J. M., 2000: Alpine glacier and pluvial lake records of late Pleistocene climate variability in the western United States. Ph.D. thesis, Oregon State University, 150 pp.
- , P. U. Clark, J. W. Jenson, and D. R. MacAyeal, 1998: Deglaciation of a soft-bedded Laurentide Ice Sheet. *Quat. Sci. Rev.*, **17**, 427–448.
- Lighty, R. G., I. G. Macintyre, and R. Stuckenrath, 1982: *Acropora palmata* reef framework: A reliable indicator of sea level in the Western Atlantic for the past 10,000 years. *Coral Reefs*, **1**, 125–130.
- Middleton, R., L. Brown, B. Dezfouly Arjomandy, and F. Klein, 1993: On 10Be standards and half-life of 10Be. *Nucl. Instrum. Methods Phys. Res.*, **82**, 399–403.
- Miller, G. H., A. P. Wolfe, J. P. Briner, P. E. Sauer, and A. Nesje, 2005: Holocene glaciation and climate evolution of Baffin Island, Arctic Canada. *Quat. Sci. Rev.*, **24**, 1703–1721.
- Mitchell, J. F. B., N. S. Grahame, and K. J. Needham, 1988: Climate simulations for 9000 years before present: Seasonal variations and effect of the Laurentide Ice Sheet. *J. Geophys. Res.*, **93**, 8283–8303.
- Mitrovica, J. X., A. M. Forte, and M. Simons, 2000: A reappraisal of postglacial decay times from Richmond Gulf and James Bay, Canada. *Geophys. J. Int.*, **142**, 783–800.
- Montaggioni, L., G. Cabioch, G. Camoin, E. Bard, A. Ribaud-Laurenti, G. Faure, P. Déjardin, and J. Récy, 1997: Continuous record of reef growth over the past 14 ky on the mid-Pacific island of Tahiti. *Geology*, **25**, 555–558.
- Pollard, D., J. C. Bergengren, L. M. Stillwell-Soller, B. Felzer, and S. L. Thompson, 1998: Climate simulations for 10,000 and 6,000 years BP. *Paleoclimates*, **2**, 183–218.
- Raisbeck, G. M., F. Yiou, D. Bourlès, E. T. Brown, D. Deboffle, P. Jouhannau, J. Lestringuez, and Z. Q. Zhou, 1994: The AMS facility at Gif-sur-Yvette: Progress, perturbations and projects. *Nucl. Instrum. Methods Phys. Res.*, **92**, 43–46.
- Renssen, H., H. Goosse, T. Fichefet, V. Brovkin, E. Driesschaert, and F. Wolk, 2005: Simulating the Holocene climate evolution at northern high latitudes using a coupled atmosphere-sea ice-ocean-vegetation model. *Climate Dyn.*, **24**, 23–43.
- Rinterknecht, V. R., 2003: Cosmogenic ¹⁰Be Chronology for the

- Last Deglaciation of the Southern Scandinavian Ice Sheet. Ph.D. thesis, Oregon State University, 99 pp.
- , P. U. Clark, G. M. Raisbeck, F. Yiou, E. J. Brook, S. Tschudi, and J. P. Lunkka, 2004: Cosmogenic ^{10}Be dating of the Salpausselkä I Moraine in southwestern Finland. *Quat. Sci. Rev.*, **23**, 2283–2289.
- Short, S. K., and H. Nichols, 1977: Holocene pollen diagrams from subarctic Labrador-Ungava: Vegetational history and climate change. *Arct. Alp. Res.*, **9**, 265–290.
- Solignac, S., A. de Vernal, and C. Hillaire-Marcel, 2004: Holocene sea-surface conditions in the North Atlantic—Contrasted trends and regimes in the western and eastern sectors (Labrador Sea vs. Iceland Basin). *Quat. Sci. Rev.*, **23**, 319–334.
- Stone, J. O., 2000: Air pressure and cosmogenic isotope production. *J. Geophys. Res.*, **105**, 23 753–23 759.
- , G. A. Balco, D. E. Sugden, M. W. Caffee, L. C. Sass III, S. G. Cowdery, and C. Siddoway, 2003: Holocene deglaciation of Marie Byrd Land, West Antarctica. *Science*, **299**, 99–102.
- Veillette, J. J., A. S. Dyke, and M. Roy, 1999: Ice-flow evolution of the Labrador Sector of the Laurentide Ice Sheet: A review, with new evidence from northern Quebec. *Quat. Sci. Rev.*, **18**, 993–1019.